

# Binding affinities analysis of ivermectin, nucleocapsid and ORF6 proteins of SARS-CoV-2 to human importins $\alpha$ isoforms: A computational approach

Análisis de las afinidades de unión de la ivermectina, las proteínas nucleocápside y ORF6 del SARS-CoV-2 a las isoformas de las importinas  $\alpha$  humanas: Un enfoque computacional

Elvio Gayozo<sup>1,4\*</sup>, Laura Rojas<sup>2,4</sup> and Julio Barrios<sup>3,4</sup>

<sup>1</sup> National University of Asunción, Faculty of Exact and Natural Sciences, Department of Biology, San Lorenzo, Paraguay.

<sup>2</sup> National University of Asunción, Faculty of Chemical Sciences, Department of Industrial Microbiology, San Lorenzo, Paraguay.

<sup>3</sup> National University of Asunción, Health Sciences Research Institute, San Lorenzo, Paraguay.

<sup>4</sup> Faculty of Exact and Natural Sciences, Grupo de Investigación en Toxicología, Genética y Bioinformática (GITGeBio), San Lorenzo, Paraguay.

## ABSTRACT

Ivermectin has been shown *in vitro* that reduces SARS-CoV-2 replication in infected cells through interactions with importins  $\alpha$ , however, the exact mechanism of action is still unknown. The objective of this study was to analyze binding affinities of ivermectin, SARS-CoV-2 nucleocapsid (N) and ORF6 proteins, to isoforms of human importins  $\alpha$  using molecular docking methods. Crystallized structures of importins  $\alpha$  from Protein Data Bank (PDB) and AlphaFold Protein Structure Database were used, viral proteins were modeled using AlphaFold 2. Molecular docking simulations were performed between human importin  $\alpha$  isoforms, ivermectin, N and ORF6 proteins, employing Broyden-Fletcher-Goldfarb-Shanno, FTDock and pyDockRST algorithms. Obtained data evidenced that viral proteins of SARS-CoV-2 and ivermectin showed favorable binding affinities to ARM2-ARM4 domains (major binding site), sharing binding affinities to the same active residues. These results suggest that ivermectin shares the same active site on the  $\alpha$ -importins as the SARS-CoV-2 N and ORF6 proteins, demonstrating a potential molecular target for research in the development of new antiviral drugs against COVID-19.

**Keywords:** Antiparasitic agent, cheminformatics, COVID-19, karyopherins, viral proteins.

## RESUMEN

Se ha demostrado *in vitro* que la ivermectina reduce la replicación del SARS-CoV-2 en células infectadas mediante la interacción con importinas  $\alpha$ , sin embargo, aún se desconoce el mecanismo exacto de acción. El objetivo de este estudio fue analizar afinidades de unión de la ivermectina, la nucleocápside (N) y las proteínas ORF6 del SARS-CoV-2 con isoformas de importinas  $\alpha$  humanas utilizando métodos de acoplamiento molecular. Se utilizaron estructuras cristalizadas de importinas  $\alpha$  de Protein Data Bank (PDB) y de la AlphaFold Protein Structure Database, y las proteínas virales se modelaron utilizando AlphaFold 2. Se llevaron a cabo simulaciones de acoplamiento molecular entre isoformas de la importina  $\alpha$

humana, la ivermectina, y las proteínas N y ORF6, empleando los algoritmos Broyden-Fletcher-Goldfarb-Shanno, FTDock y pyDockRST. Los datos obtenidos evidenciaron que las proteínas virales del SARS-CoV-2 y la ivermectina presentan afinidades de unión favorables a los dominios ARM2-ARM4 (sitio principal de unión), compartiendo afinidades de interacción con los mismos residuos activos. Estos resultados sugieren que la ivermectina comparte el mismo sitio activo en las importinas  $\alpha$  que las proteínas N y ORF6 de SARS-CoV-2, demostrando una potencial diana molecular para la investigación en el desarrollo de nuevos fármacos antivirales contra la COVID-19.

**Palabras clave:** Antiparasitario, quimioinformática, COVID-19, carioferinas, proteínas virales.

## INTRODUCTION

SARS-CoV-2 genome analysis has revealed between 79.6 % to 80 % of genetic identity with SARS-CoV, showing similarities in proteins encoding sequences and viral infection mechanism (Andersen *et al.*, 2020; Shereen *et al.*, 2020; Wu *et al.*, 2020; Zhou *et al.*, 2020). Genomic study showed a close phylogenetic relationships between SARS-CoV-2 and SARS-CoV genomes, suggesting a similar evolutionary origin, however, SARS-CoV-2 has better host adaptation (Chen *et al.*, 2021).

Keys proteins for a successful replication have been reported in both viruses, the nucleocapsid protein (N) and ORF6 protein (Kopecky-Bromberg *et al.*, 2007; Gao *et al.*, 2021). Nucleocapsid protein plays crucial roles such as viral genome protection and traffic to exocytic vesicles, but the crucial function is blocking interferon-mediated antiviral response (Shereen *et al.*, 2020; Li *et al.*, 2020; Iqbal *et al.*, 2020; Kannan *et al.*, 2020; Kopecky-Bromberg *et al.*, 2007; Qinfen *et al.*, 2004; Rowland *et al.*, 2005; Timani *et al.*, 2005; Surjit *et al.*, 2004). A recent study suggests as a possible subcellular localization for SARS-CoV-2 N protein, the nucleus of the host cell (Gao *et al.*, 2021). The presence of N proteins in the nucleus/

\*Author for correspondence: Elvio Gayozo

e-mail: elviologo@gmail.com

Received: October 24, 2024

Accepted: February 21, 2025

Published: March 13, 2025

nucleolus of infected cells has been described in SARS-CoV infection, due to structural exposure of nuclear localization sequences (NLS) in regions of the C-terminal domain, which is recognized by importins  $\alpha$  (Timani *et al.*, 2005; He *et al.*, 2004; Wulan *et al.*, 2015; Wurm *et al.*, 2001).

ORF6 protein in coronaviruses is intimately related to importins  $\alpha$  functions, specifically to importin  $\alpha 1$ , but the presence of this protein inside the host nucleus has not been evidenced yet (Gordon *et al.*, 2020; Frieman *et al.*, 2007; Hussain and Gallagher, 2010; Zhao *et al.*, 2009). ORF6 and N proteins are essential for the inhibition of the interferon signaling pathway during infection with both viruses (SARS-CoV and SARS-CoV-2) (Frieman *et al.*, 2007; Li *et al.*, 2020; Liu *et al.*, 2014; Ye *et al.*, 2008; Zhao *et al.*, 2009).

Importins  $\alpha$  are responsible to NLS recognition in proteins that will be transported into the nucleus, playing an important role mediating antiviral responses through STAT1/STAT2 pathway (Pumroy and Cingolani, 2015). Several studies have shown that viruses are able to use this cellular transport pathway, specifically to import viral proteins into the nucleus and to block antiviral response mechanism of infected cells (Gayozo and Rojas, 2021; Pumroy and Cingolani, 2015).

An *in vitro* study has shown that ivermectin is able to decrease the SARS-CoV-2 viral genome load about 5000 fold in 48 hours post-treatment, the researchers suggest via blockage in the trafficking of viral proteins between nucleoplasm and cytoplasm (Caly *et al.*, 2020). One of the key mechanisms of action reported for ivermectin molecules against SARS-CoV-2 infection is the binding affinity to importin  $\alpha/\beta 1$  heterodimers, as well as for other karyopherins (KPNA/KPNB) receptors, inhibiting viral protein transport into the nucleus of the infected cell, however, it is still unknown how protein transport inhibition acts against SARS-CoV-2 proteins translocation (Zaidi and Dehgani-Mobaraki, 2022).

Due to this, protein-protein and protein-ligand molecular docking simulation were performed between ivermectin, N and ORF6 proteins of SARS-CoV-2, to human importins  $\alpha$  isoforms as main target. In addition to this, active residues, molecular interactions in complexes were identified to understand the interactions modes between ivermectin, SARS-CoV-2 N and ORF6 proteins to importins  $\alpha$  isoforms encoded in human genome, and to recognize possible molecular targets for the development of new antivirals against COVID-19.

## MATERIAL AND METHODS

### Analysis of similarities between N and ORF6 proteins sequences

Nucleocapsid amino acid sequences of SARS-CoV-2, SARS-CoV, MERS-CoV, HCoV-OC43, HCoV-NL63, HCoV-HKU1, HCoV-229E and the ORF6 protein sequences of SARS-CoV-2 and SARS-CoV, belonging to *Coronaviridae* family, were obtained from the NCBI (*National Center for Biotechnology Information*, <https://www.ncbi.nlm.nih.gov/>) database (Table 1). These sequences were selected taking into account the infectious capacity of the most common coronaviruses that affect humans and the degree of conservation of the sequences, following the methodology proposed by Ibrahim *et al.* (2020).

**Table 1.** Accession code of N and ORF6 proteins sequences.

**Tabla 1.** Código de acceso de las secuencias de las proteínas N y ORF6.

Virus	Accession code	Database
<b>Nucleocapsid protein</b>		
SARS-CoV-2	QHO62110.1	NCBI (Protein)
SARS-CoV	ABA02277.1	NCBI (Protein)
MERS-CoV	AZK15907.1	NCBI (Protein)
HCoV-OC43	QBP84763.1	NCBI (Protein)
HCoV-NL63	ABE97134.1	NCBI (Protein)
HCoV-HKU1	ARU07581.1	NCBI (Protein)
HCoV-229E	ARU07605.1	NCBI (Protein)
<b>ORF6 Protein</b>		
SARS-CoV-2	QIV65092.1	NCBI (Protein)
SARS-CoV	NP_828856.1	NCBI (Protein)

Relationships between proteins sequences were determined by phylogenetic reconstruction, using neighbor joining method with a bootstrap of 1000 replicates and Poisson substitution model using MEGA X software (Kumar *et al.*, 2018). Alignment between amino acid sequences were performed using Clustal Omega algorithm (Sievers and Higgins, 2014), and BLOSUM 62 matrix between SARS-CoV-2 and SARS-CoV sequences to determine identity and similarity between them and record the conserved regions, for it EMBL-EBI tools (<https://www.ebi.ac.uk/jdispatcher/psa>) (Li *et al.*, 2015) and ESPript 3.0 software were used (Robert and Gouet, 2014).

### Detection of nuclear localization sequences (NLS) and hydrophobicity analysis

The search for putative NLS sequences, according to animal cell code, in the SARS-CoV-2 N and ORF6 proteins sequences was performed using WoLF PSORT tool (<https://wolfpsort.hgc.jp/>) (Horton *et al.*, 2007), in order to identify possible putative regions targeting importins  $\alpha$  (Fang *et al.*, 2017).

Hydrophobic content analysis of ORF6 protein of SARS-CoV-2 and SARS-CoV was performed calculating GRAVY hydrophobicity index and constructing hydrophobicity plot according to Kyte and Doolittle index (Kyte and Doolittle, 1982). This analysis was performed in order to characterize the ORF6 protein of both viruses and to establish similarities in terms of possible transmembrane regions with  $\alpha$ -helix structures (Fry *et al.*, 2021).

### Molecular docking protein-protein simulations

Molecular modeling of ORF6 protein structure (NCBI: QIV65092.1) was performed using AlphaFold 2 (Jumper *et al.*, 2021; Mirdita *et al.*, 2022). Modeled structure was validated using MolProbity 4.5.1, PROCHECK and Chimera v. 1.16 software (Laskowski *et al.*, 1993; Pettersen *et al.*, 2004; Williams *et al.*, 2018). The acceptance criteria for statistical and structural values are described in the Supplementary Figure S1.

The molecular structure of SARS-CoV-2 N protein (PDB: 8FD5), and importins  $\alpha$  isoforms of the  $\alpha 1$  subfamily (isoforms  $\alpha 1$  and  $\alpha 8$ ),  $\alpha 2$  subfamily (isoforms  $\alpha 3$  and  $\alpha 4$ ) and  $\alpha 3$  subfamily (isoforms  $\alpha 5$ ,  $\alpha 6$  and  $\alpha 7$ ) were obtained from

Protein Data Bank RCSB database (<https://www.rcsb.org/>) and AlphaFold Protein Structure Database (<https://alphafold.ebi.ac.uk/>) (Berman *et al.*, 2000; David *et al.*, 2022; Varadi *et al.*, 2022) (Table 2).

Molecular protein-protein docking simulations were performed employing Ibrahim *et al.* (2020) bioinformatic workflow, these assays were carried out between N protein and importin  $\alpha$  isoforms, and between ORF6 protein and isoform importin  $\alpha 1$ , for it were used pyDock 3 software (Cheng *et al.*, 2007). To select the complex with favorable binding affinities, were employed electrostatic, desolvation and van der Waals energies values (Cheng *et al.*, 2007; Grosdidier *et al.*, 2007; Jiménez-García *et al.*, 2013; Pallara *et al.*, 2017). Water molecules, ions and ligands were firstly removed from protein structures (Chook and Blobel, 2001).

Simulations were performed using receptor-ligand model generated by FTDock (Fourier Transform Dock) and pyDockRST algorithms (Chelliah *et al.*, 2006; Cheng *et al.*, 2007; Gabb *et al.*, 1997; Grosdidier *et al.*, 2007; Jiménez-García *et al.*, 2013). Firstly, polar hydrogens were added at physiological pH 7.4, and also partial charges were incorporated to the protein structures using CHARMM force field, using the Discovery Studio Visualizer v. 20 software (Biovia Dassault Systemes, USA). Restraints distances methods were employed in importins  $\alpha$  active sites (major binding site and minor binding site) corresponding to Armadillo (ARM) domains (ARM2, ARM3, ARM4, ARM6, ARM7, ARM8) (Chook and Blobel, 2001).

Resulting complexes were subjected to structural refinement process using 14.4 ps molecular dynamics simulation methods with GalaxyRefineComplex software (Heo *et al.*, 2016). Free binding energy ( $\Delta G$ ) of complexes was calculated at 37° C (310.15 K) using PRODIGY software (Vangone *et al.*, 2019).

Identification of active residues and intermolecular forces was performed using tridimensional (3D) and bidimensional (2D) representations, employing CHARMM force fields method with Discovery Studio Visualizer v. 20 software (Biovia Dassault Systemes, USA).

**Table 2.** Structures of the importin  $\alpha$  isoforms used in this research.

**Tabla 2.** Estructuras de las isoformas de importina  $\alpha$  utilizadas en esta investigación.

Subfamily	Isoforms	Accession code	Database
$\alpha 1$	Importin $\alpha 1$	4WV6	Protein Data Bank RCSB
	Importin $\alpha 8$	A9QM74	AlphaFold Protein Structure Database
$\alpha 2$	Importin $\alpha 3$	4UAE	Protein Data Bank RCSB
	Importin $\alpha 4$	O00505	AlphaFold Protein Structure Database
$\alpha 3$	Importin $\alpha 5$	P52294	AlphaFold Protein Structure Database
	Importin $\alpha 6$	O15131	AlphaFold Protein Structure Database
	Importin $\alpha 7$	4UAD	Protein Data Bank RCSB

## Molecular docking protein-ligand simulations

The molecular structure of ivermectin (ivermectin B1a) (PubChem CID Code: 6321424) was obtained from PubChem Database (<https://pubchem.ncbi.nlm.nih.gov/>) (Kim *et al.*, 2016).

Energetic minimization of ivermectin structure was performed with Merck Molecular Force Field 94 (MMFF94) method, using for it, five steps per update with conjugate gradient algorithm, a total cycle number of 50000 steps, an energy convergence criteria of 0.001 kcal.mol<sup>-1</sup>.Å<sup>-1</sup>, also partial charges with Gasteiger force field and polar hydrogen atoms at physiological pH of 7.4 were added using Avogadro 2 software (Hanwell *et al.*, 2012) and Chimera v. 1.16 software (Pettersen *et al.*, 2004).

Molecular docking simulations between ivermectin and importin  $\alpha$  isoforms were performed in a grid with dimensions of 43x73x78 Å<sup>3</sup>, 50 iterations in simulations and an exhaustiveness of 16, using PyRx software (Dallakyan and Olson, 2015) and Autodock Vina software (Trott and Olson, 2010).

Visualization of complexes, identification of binding site, active residues and intermolecular forces was performed employing CHARMM force fields and Momany-Rone partial charge, for it Discovery Studio Visualizer v. 20 software (Biovia Dassault Systemes, USA) was used.

## RESULTS AND DISCUSSION

### N proteins sequences analysis

Phylogenetic reconstruction reveals a close relationship between the SARS-CoV-2 N protein and SARS-CoV N protein sequences in a 94 % of the analysis (Figure 1.A).

Results obtained in phylogenetic reconstruction are in agreement with genetic similarity reported in another research where an identity of 79.6 % to 80 % between both genomes was found (Ceraolo and Giorgi, 2020; Lu *et al.*, 2020; Wu *et al.*, 2020; Zhou *et al.*, 2020). Kannan *et al.* (2020) and Ceraolo and Giorgi (2020) also described a high percentage of identity between amino acid sequences of nucleocapsid protein of SARS-CoV-2 and SARS-CoV, these authors suggest a 90 % to 90.52 % identity between these viral genomes, differences were registered in residues Gly25, Ser26, Asp103, Ala217 and Thr334, which were part of 380 residues substituted in the SARS-CoV-2 proteome (Wu *et al.*, 2020) (Figure 2).

This sequences relationships suggests structural and functional similarities such as the ability to suppress Interferon Stimulation Response Element (ISRE) gene expression, that was also reported for other coronaviruses (Li *et al.*, 2020; Kannan *et al.*, 2020; Ceraolo and Giorgi, 2020; Chang *et al.*, 2014; Timani *et al.*, 2005) (Figure 1.A).

However, the analysis of SARS-CoV-2 N protein sequence showed the presence of a monopartite NLS sequence pat 4 "KKPR" (Lys-Lys-Pro-Arg) between residues 256-259, and a monopartite sequence of pat 7 "PKKDKKKK" (Pro-Lys-Lys-Asp-Lys-Lys-Lys-Lys) between residues 368-375 (Figure 1.B).

The NLS sequences detected in SARS-CoV-2 N protein are similar to those described in SARS-CoV N protein, howe-

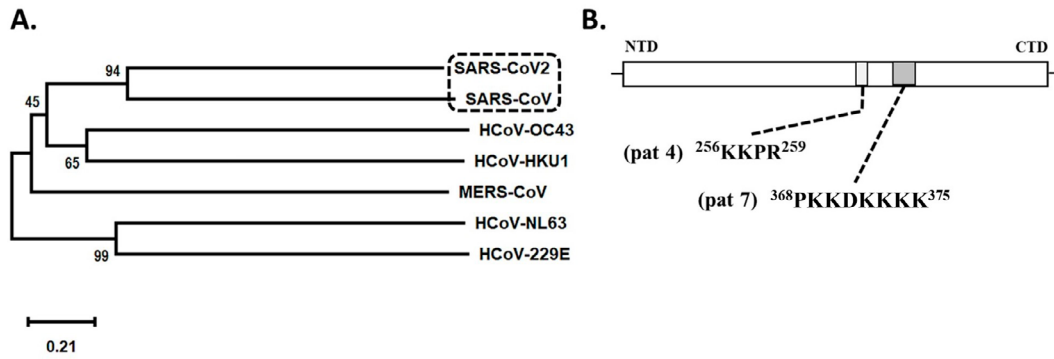


**Figure 1. A.** Phylogenetic reconstruction from amino acid sequences of nucleocapsid proteins. **B.** Representation of SARS-CoV-2 Nucleocapsid protein and SLN sequences, NTD: N-Terminal Domain, CTD: C-Terminal Domain.

**Figura 1. A.** Reconstrucción filogenética a partir de las secuencias de aminoácidos de las proteínas de la nucleocápside. **B.** Representación de la proteína nucleocápside del SARS-CoV-2 y secuencias SLN, NTD: Dominio N-Terminal, CTD: Dominio C-Terminal.

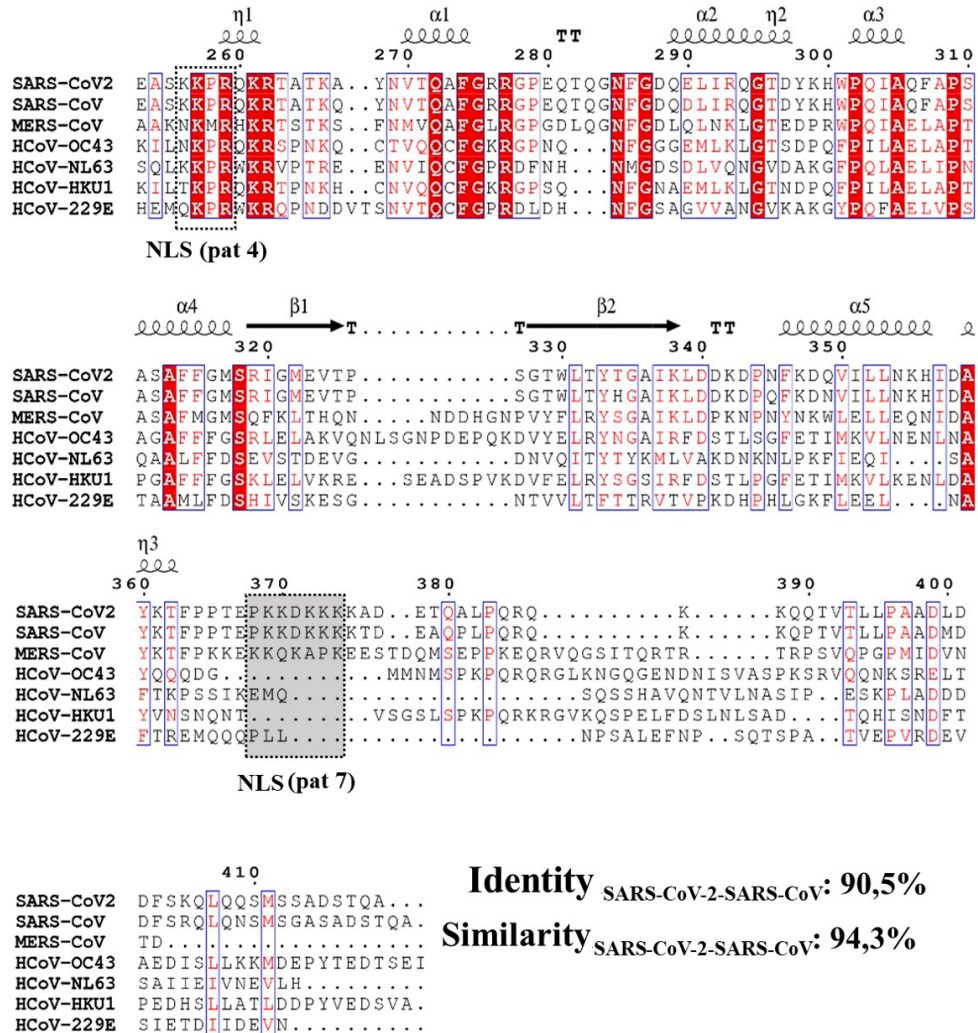


**Figure 2.** Multiple amino acid sequence alignment of viral nucleocapsid protein. NLS pat4 sequences and NLS pat7 sequences highlighted.

**Figura 2.** Alineación múltiple de secuencias de aminoácidos de la proteína nucleocápside viral. Secuencias NLS pat4 y NLS pat7 resaltadas.

ver, in SARS-CoV a third NLS monopartite pat 7 sequence was recorded next to N-terminal domain between residues 38 to 44, which is absent in SARS-CoV-2 N protein due to substitution of residue 38 for a serine. The presence of NLS sequence next to the N-terminal domain of the SARS-CoV N-protein is functional, leading an exogenous protein into the nucleus, however it seems to be not relevant for the success of viral infection, becoming more important NLS sequences close to the C-terminal domain (Timani *et al.*, 2005).

The similarity between SARS-CoV and SARS-CoV-2 N proteins is clearly visible in the multiple alignment representation, where a 90.5 % of identity and a 94.3 % of similarity between these two sequences were recorded (Figure 2).

Previous studies reported that SARS-CoV N proteins are cleaved during activation of caspases 3 and 7, that induce apoptosis in infected cells, generating fragments with functional NLS sequences that facilitate translocation of these fragments into the nucleus/nucleolus (He *et al.*, 2004; Rowland *et al.*, 2005; Timani *et al.*, 2005).

It is important to mention that proteins fragments translocations into the nucleus occurs in low proportions at advanced stages of SARS-CoV infection, and that because the multimerization of N proteins blocks the cleavages (He *et al.*, 2004; Timani *et al.*, 2005). The presence of NLS sequences in SARS-CoV-2 N protein was also described by Gao *et al.* (2021).

**Protein-protein molecular docking simulations of N protein and importin  $\alpha$  isoforms**

Molecular docking analysis evidenced binding affinities of the N proteins (NLS pat4, NLS pat7) to the ARM2-ARM4 domains of the evaluated importins  $\alpha$  isoforms, these domains correspond to the major binding site, a NLS recognition site in importins (Baumhardt and Chook, 2018; Chook and Blobel, 2001) (Figure 3, Figure 4). It is important to denote that the entry of peptides/proteins with NLS sequences into the nuclear compartment occurs by classical importin  $\alpha$  mediated pathway, NLS sequences possess the ability to interact with ARM domains of importins  $\alpha$  (Chook and Blobel, 2001).

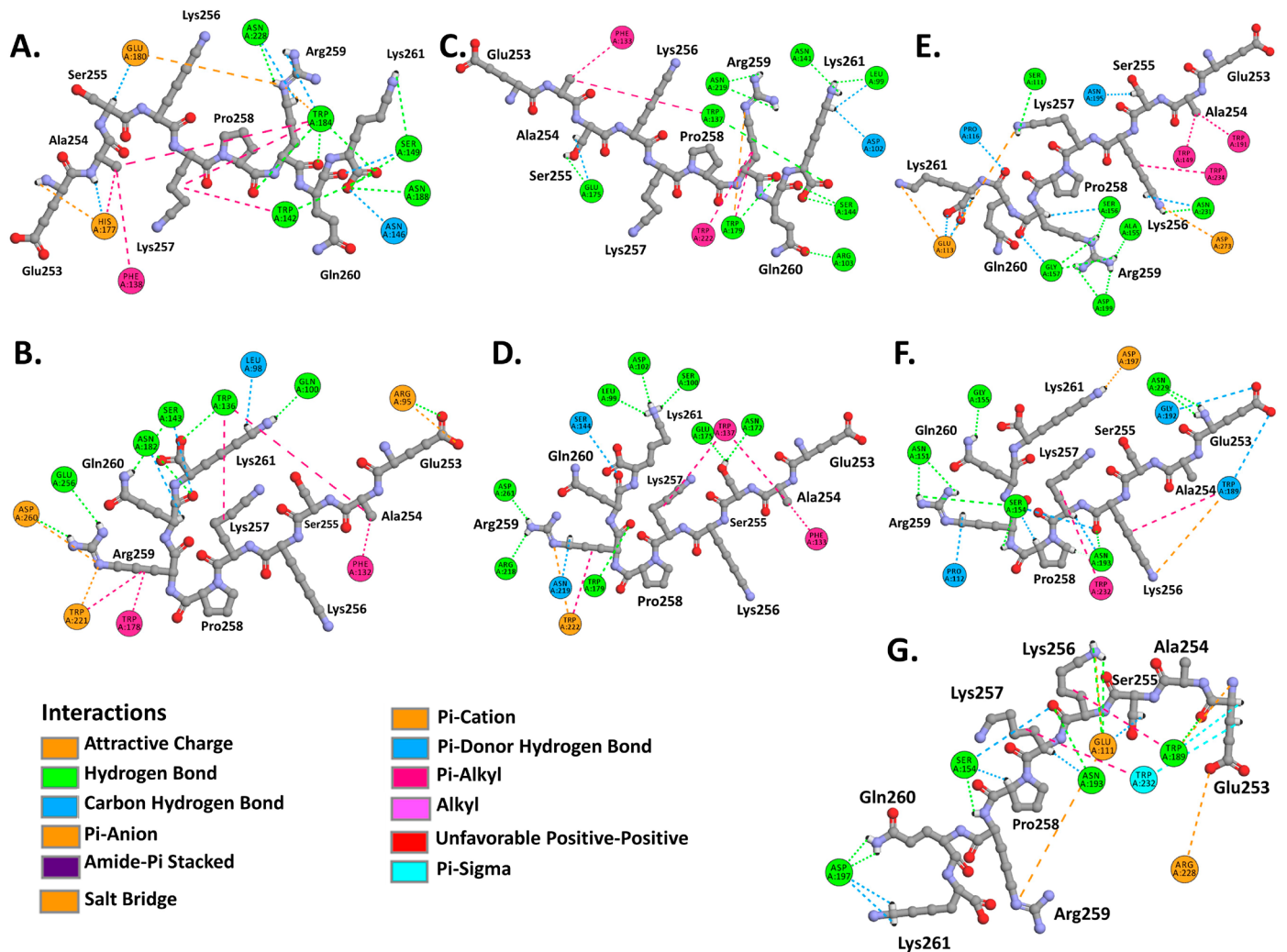


**Figure 3.** Complexes of SARS-CoV-2 protein N (NLS pat4) and  $\alpha$  importins isoforms. **A.** Importin  $\alpha$ 1. **B.** Importin  $\alpha$ 8. **C.** Importin  $\alpha$ 3. **D.** Importin  $\alpha$ 4. **E.** Importin  $\alpha$ 5. **F.** Importin  $\alpha$ 6. **G.** Importin  $\alpha$ 7.

**Figura 3.** Complejos de la proteína N (NLS pat4) del SARS-CoV-2 y las isoformas  $\alpha$  de las importinas. **A.** Importina  $\alpha$ 1. **B.** Importina  $\alpha$ 8. **C.** Importina  $\alpha$ 3. **D.** Importina  $\alpha$ 4. **E.** Importina  $\alpha$ 5. **F.** Importina  $\alpha$ 6. **G.** Importina  $\alpha$ 7.

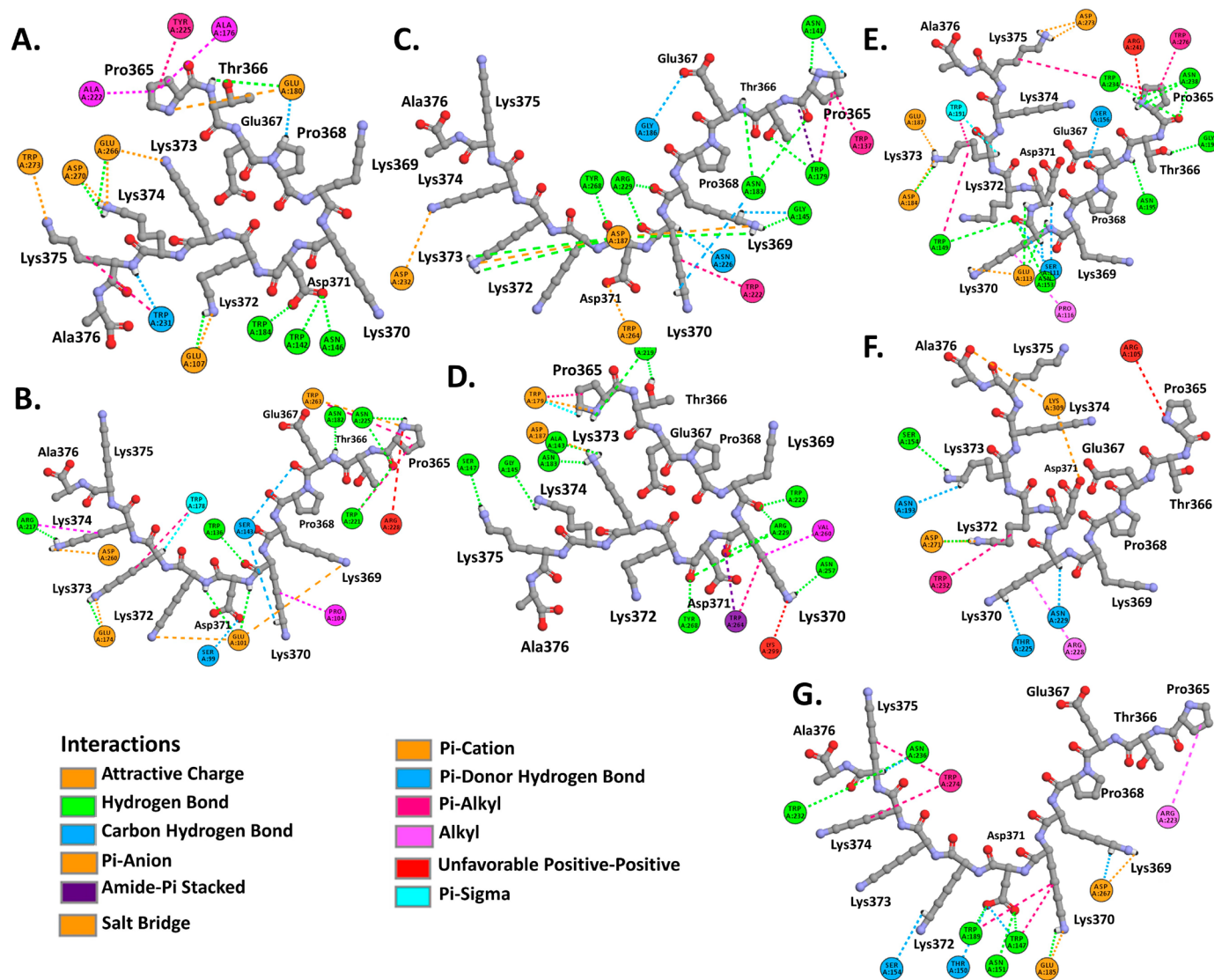


**Figure 4.** Complexes of SARS-CoV-2 protein N (NLS pat7) and importin  $\alpha$  isoforms. **A.** Importin  $\alpha 1$ . **B.** Importin  $\alpha 8$ . **C.** Importin  $\alpha 3$ . **D.** Importin  $\alpha 4$ . **E.** Importin  $\alpha 5$ . **F.** Importin  $\alpha 6$ . **G.** Importin  $\alpha 7$ .

**Figura 4.** Complejos de proteína N (NLS pat7) de SARS-CoV-2 e isoformas de importina  $\alpha$ . **A.** Importina  $\alpha 1$ . **B.** Importina  $\alpha 8$ . **C.** Importina  $\alpha 3$ . **D.** Importina  $\alpha 4$ . **E.** Importina  $\alpha 5$ . **F.** Importina  $\alpha 6$ . **G.** Importina  $\alpha 7$ .

Resulting complexes between importins  $\alpha$  isoforms and N protein (NLS pat4 and pat7) showed free binding energy values ( $\Delta G$ ) ranging  $-10.0$  to  $-6.3$  kcal.mol $^{-1}$ , where the NLS pat7 sequence demonstrated the most favorable energy value, specifically to importin  $\alpha 3$  and importin  $\alpha 5$  (Figure 3.B, Supplementary Table S1).

Active residues in complexes formed by N protein and isoforms of  $\alpha 1$  subfamily were Phe138, Trp142, Asn146, Ser149, His177, Glu180, Trp184, Asn188, Asn228 in importin  $\alpha 1$ , and Arg95, Gln100, Glu107, Trp136, Ser143, Glu180, Asn182, Trp231, Glu256, Asp260, Glu266, Asp270, Trp273 in importin  $\alpha 8$ , residues that interact with NLS pat4 sequences through hydrogen bonds, unconventional interactions between a polarized carbon atom and hydrogen atom, interactions between Pi orbitals and donors groups of hydrogen bonds. The formation of electrostatic attractions and

hydrophobic interactions were also identified (Figure 3.A,B, Supplementary Figure S2, Supplementary Figure S3, Supplementary Table S1).

Residues Glu107, Trp142, Asn146, Ala176, Glu180, Trp184, Ala222, Tyr225, Trp231, Glu266, Asp270, Trp273 of importin  $\alpha 1$ , and residues Ser99, Glu101, Pro104, Trp136, Ser143, Arg217, Asp260, Trp263, Glu174, Trp178, Asn182, Trp221, Asn225 of importin  $\alpha 8$ , interact by hydrogen bonds, carbon hydrogen bonds, Pi interactions with hydrogen bonds donors, hydrophobic and electrostatic interactions with the NLS pat7 sequences (Figure 4.A,B, Supplementary Figure S2, Supplementary Figure S3, Supplementary Table S1).

Complexes formed by  $\alpha 2$  subfamily isoforms revealed as active residues to Leu99, Asp102, Arg103, Phe133, Trp137, Asn141, Ser144, Trp179, Glu175, Asn219, Trp222 in importin  $\alpha 3$ , Leu99, Ser100, Asp102, Phe133, Trp137, Ser144, Asn172,

Glu175, Trp179, Arg218, Asn219, Trp222, Asp261 in importin  $\alpha$ 4, all of them interacting with the NLS pat4 sequences, exhibiting hydrogen bonds, carbon hydrogen bonds, electrostatic and hydrophobic interactions (Figure 3.C,D, Supplementary Figure S2, Supplementary Figure S3, Supplementary Table S1).

Also registered as active residues were Trp179, Asn183, Gly186, Asp187, Asn219, Trp222, Asn226, Arg229, Asp232, Trp137, Asn141, Ala143, Gly145, Ser147, Asn257, Val260, Trp264, Tyr268 in importin  $\alpha$ 3, and Ala143, Gly145, Ser147, Trp179, Asn183, Asp187, Asn219, Trp222, Arg229, Asn257, Val260, Trp264, Tyr268 in importin  $\alpha$ 4, which interact with NLS pat7 sequences (Figure 4.C,D, Supplementary Figure S2, Supplementary Figure S3, Supplementary Table S1).

Complexes registered with  $\alpha$ 3 subfamily isoforms showed as active residues to Ser111, Glu113, Pro116, Trp149, Ala155, Ser156, Gly157, Trp191, Asn195, Asp199, Asn231, Trp234, Asp273 of importin  $\alpha$ 5, and Pro112, Asn151, Ser154, Trp189, Gly192, Asn193, Asp197, Asn229, Trp232 of importin  $\alpha$ 6, and Glu111, Ser154, Trp189, Asn193, Asp197, Arg228, Trp232 in importin  $\alpha$ 7, all these residues interact with NLS pat4 sequences by hydrogen bonds, carbon hydrogen interactions, electrostatic attractions and hydrophobic inte-

ractions (Figure 3.E,F,G, Supplementary Figure S2, Supplementary Figure S3, Supplementary Table S1).

Also, residues Ser111, Glu113, Pro116, Trp149, Asn153, Ser156, Asp184, Glu187, Trp191, Asn195, Gly198, Trp234, Asn238, Asp273, Trp276 in importin  $\alpha$ 5, Ser154, Asn193, Thr225, Arg228, Asn229, Trp232, Asp271, Lys309 in importin  $\alpha$ 6, Trp147, Thr150, Asn151, Ser154, Glu185, Trp189, Arg223, Trp232, Asn236, Asp267, Trp274 in importin  $\alpha$ 7, were detected in interactions with NLS pat7 sequences (Figure 4.E,F,G, Supplementary Figure S2, Supplementary Figure S3, Supplementary Table S1).

**ORF6 proteins sequences analysis**

Amino acid sequences of SARS-CoV and SARS-CoV-2 ORF6 proteins showed 66.7 % of identity and 85.7 % of similarity among them (Figure 5.A).

These proteins present high hydrophobicity scores in the Kyte and Doolittle scale (Kyte and Doolittle, 1982), evidencing hydrophobic regions in 72.13 % of the SARS-CoV-2 ORF6 protein, suggesting the presence of an  $\alpha$ -helix transmembrane structure (between residues 1-44) (Hussain and Gallagher, 2010). The high content of residues with hydrophobic properties were evidenced in both proteins, which

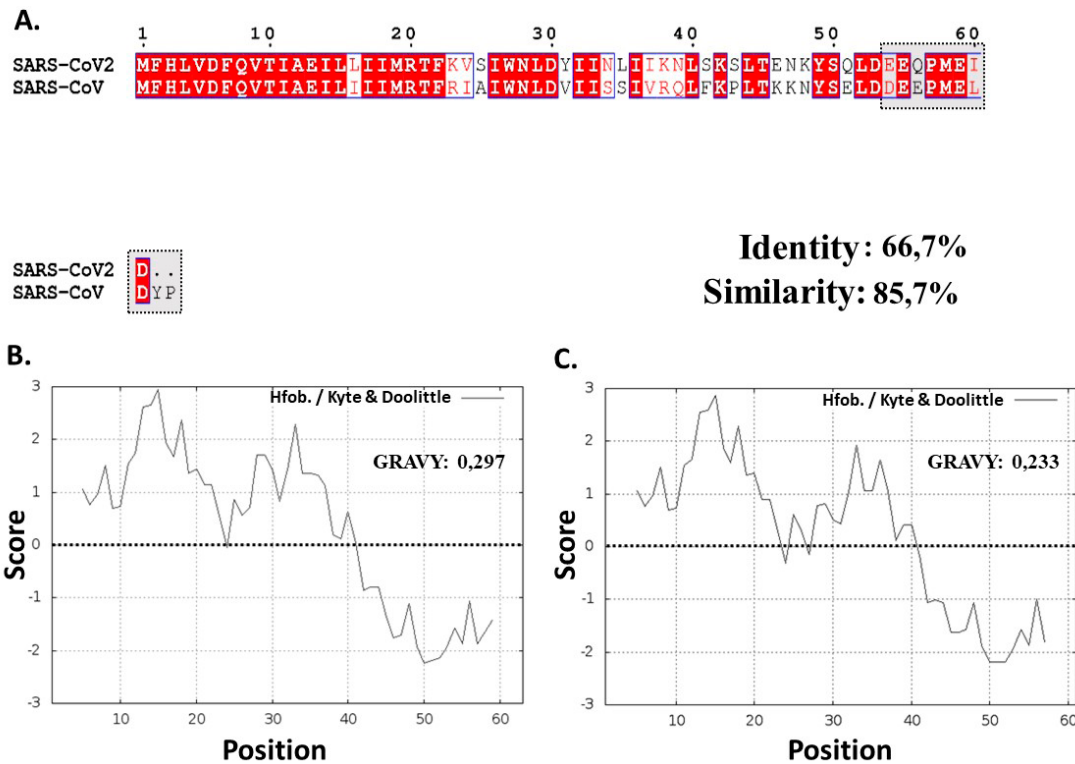


**Figure 5. A.** Alignment of SARS-CoV and SARS-CoV-2 ORF6 protein sequences, importin  $\alpha$ 1 binding segment highlighted. **B-C.** Hydrophobicity plot and index of viral ORF6 according to Kyte & Doolittle (1982). **B.** SARS-CoV ORF6 protein. **C.** SARS-CoV-2 ORF6 protein.  
**Figura 5. A.** Alineación de las secuencias de las proteínas ORF6 de SARS-CoV y SARS-CoV-2, segmento de unión a importina  $\alpha$ 1 resaltado. **B-C.** Diagrama de hidrofobicidad e índice de ORF6 viral según Kyte & Doolittle (1982). **B.** Proteína ORF6 del SARS-CoV. **C.** Proteína ORF6 del SARS-CoV-2.

could also be verified with GRAVY hydrophobicity index that showed values of 0.297 and 0.233, respectively (Figure 5.B,C). The presence of SARS-CoV ORF6 protein in the membrane of the endoplasmic reticulum (ER)/ Golgi of the infected cell has been described in previous research; this similarity in terms of hydrophobicity indicators could suggest the same cellular localization of SARS-CoV-2 ORF6 and the same mechanism of action against importins  $\alpha$  (Frieman *et al.*, 2007). ORF6 proteins of SARS-CoV was also described with amphipathic characteristics, this protein mainly acts as antagonist of the host cell antiviral response and participates in the acceleration of infection kinetics (Frieman *et al.*, 2007; Hussain and Gallagher, 2010; Liu *et al.*, 2014; Zhao *et al.*, 2009).

Due to their homology and high similarity, these proteins would be sharing functions mainly involved in the inhibition of ISRE promoter expression, so interferon beta (IFN- $\beta$ ) function is also affected (Kopecky-Bromberg *et al.*, 2007), these observations were reconfirmed by Li *et al.* (2020) who reported an inhibition of interferon type I signaling pathway.

The complex importin  $\alpha$ -ORF6 SARS-CoV-2 protein showed a favorable free binding energy with a value of  $-7.7$  kcal.mol $^{-1}$ . This complex demonstrated interaction of ORF6 protein C-terminal domain to the ARM2-ARM4 (major binding site) domains of importin  $\alpha$  (Baumhardt and Chook, 2018) (Figure 6).

The active residues registered in importin  $\alpha$  were Trp142, Arg101, Trp184, Arg238, Trp273, Arg315, Trp231, Ser149, Asn146 belonging to ARM2-ARM4 domains (Figure

6.A). The importin  $\alpha$ -ORF6 complex is stabilized with hydrogen bonds, carbon-hydrogen interactions, Pi orbitals and Sigma orbitals interactions, electrostatic attractions and hydrophobic interactions (Figure 6.B).

Studies revealed that SARS-CoV ORF6 protein is able to indirectly block STAT1/STAT2 proteins nuclear translocation, this occurs by interaction of this viral protein with importin  $\alpha$ , hijacking importin  $\beta$ 1 from cytoplasm to ER/Golgi membrane surface (Frieman *et al.*, 2007; Kopecky-Bromberg *et al.*, 2007; Liu *et al.*, 2014; Narayanan *et al.*, 2008; Zhao *et al.*, 2009). As described by Frieman *et al.* (2007) and Liu *et al.* (2014), the C-terminal domain (residues 54-63) of SARS-CoV ORF6 protein involved in the interaction to importin  $\alpha$ , is located within a region with similarity to residues 54-61 in SARS-CoV-2 ORF6 protein (Figure 5.A).

A recent study performed by Miyamoto *et al.* (2022), has revealed that SARS-CoV-2 ORF6 protein exhibits antagonistic effects on interferon mediated antiviral response by blocking intracellular traffic of STAT1 through interactions between viral protein and STAT1, and a high binding affinity to importins  $\alpha$ 1 of infected cells.

Another research revealed that SARS-CoV-2 ORF6 protein plays an important role in nucleocytoplasmic traffic, through an interaction to Rae1:Nup98 complex of the host cell, this event directly manipulate localization and functions of nucleoporins causing a damaged nucleocytoplasmic traffic, promoting the accumulation of RNA transporters (Addetia *et al.*, 2021; Gordon *et al.*, 2020; Kato *et al.*, 2021).

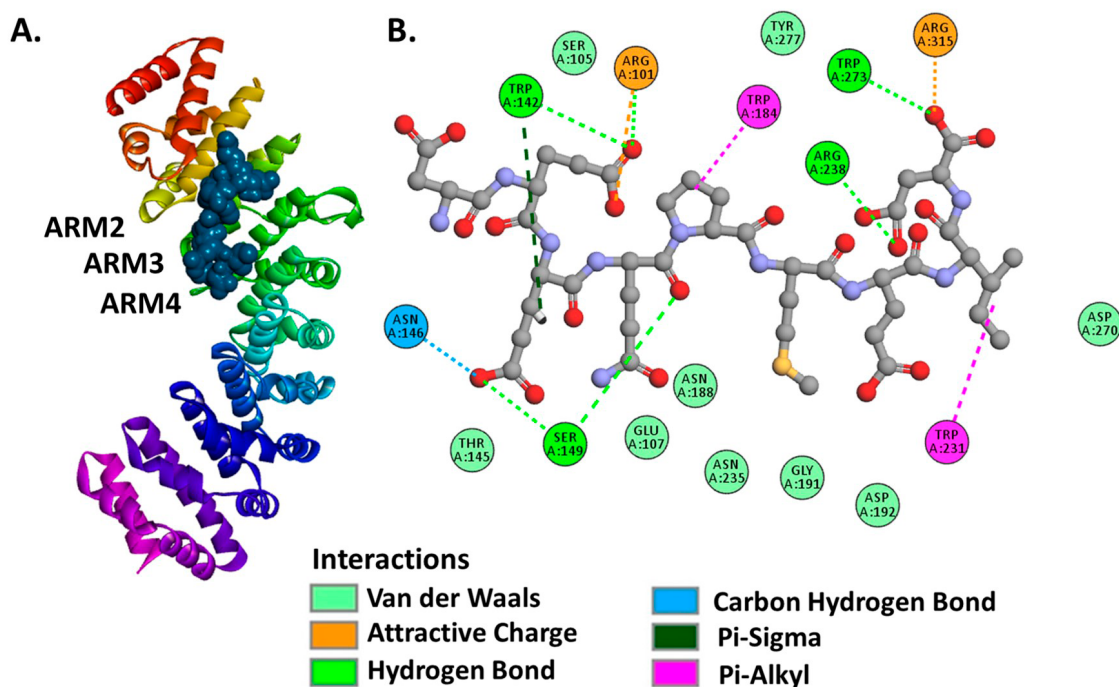


**Figure 6.** Complex of importin  $\alpha$ 1 and SARS-CoV-2 ORF6 protein. **A.** Full view of ARM domains of importin  $\alpha$ 1 binding to ORF6. **B.** Two-dimensional representation of molecular docking.

**Figura 6.** Complejo de importina  $\alpha$ 1 y proteína ORF6 del SARS-CoV-2. **A.** Vista completa de los dominios ARM de la importina  $\alpha$ 1 uniéndose a ORF6. **B.** Representación bidimensional del acoplamiento molecular.



### Protein-Ligand molecular docking simulations of ivermectin and importin $\alpha$ isoforms

Molecular docking analysis of ivermectin and importin  $\alpha$  isoforms, revealed favorable values of free binding energies ranging from  $-7.71 \pm 0.24$  to  $-8.63 \pm 0.32$  kcal.mol<sup>-1</sup>, showing a higher affinity mainly to ARM2-ARM4 domains that are topologically similar to those determined in the complexes formed by SARS-CoV-2 N protein and ORF6 proteins (Figure 3, Figure 4, Figure 7, Supplementary Table S1, Supplementary Table S2).

Active residues registered in  $\alpha 1$  subfamily isoforms were Trp142, Asn146, Trp184, Arg227, Trp231, Asn235 in importin  $\alpha 1$ , Arg217 and Trp221 in importin  $\alpha 8$ , which interact with the ivermectin molecule through hydrogen bonds and Pi-Sigma interactions (Figure 7.A,B, Supplementary Table S2).

In complexes formed by  $\alpha 2$  subfamily isoforms, active residues identified were Trp137, Glu175, Trp179, Arg218 in importin  $\alpha 3$ , and Trp137, Ser144, Asn183, Trp179 in importin  $\alpha 4$ , which interact with ivermectin by hydrogen bonds, carbon hydrogen bonds, Pi and Sigma orbitals interactions, as well as interactions between alkyl chains (Figure 7.C,D, Supplementary Table S2).

On the other hand, complexes formed with  $\alpha 3$  subfamily isoforms revealed Trp191, Gly194, Asn195, Arg230, Trp234 as active residues in importin  $\alpha 5$ , Trp189, Asp271, Trp274 in importin  $\alpha 6$ , and Gly155, Arg228, Trp232, Asn236, Trp274 in importin  $\alpha 7$ . These residues interact with ivermectin by hydrogen bonds, interactions between polarized carbon atoms and hydrogen, alkyl chains interactions, Pi and Sigma orbitals interactions, Pi orbitals and alkyl chains interactions, and interactions between Pi orbitals and donors groups of hydrogen bond (Figure 7.E,F,G, Supplementary Table S2).

Human genome encodes seven importin  $\alpha$  isoforms that are grouped into three subfamilies known as  $\alpha 1$ ,  $\alpha 2$  and  $\alpha 3$ , which share a common structure consisting in Importin  $\beta 1$  Binding domain (IBB) and ARM domains, that have the ability to interact with NLS sequences at major and minor binding sites, respectively (Pumroy and Cingolani, 2015).

Many of these isoforms have been extensively investigated due to their abilities to interact with viral proteins, this is the case of importin  $\alpha 1$ , which is a target to several viral proteins such as E1A of Adenovirus, N protein of Hantavirus, integrase and Vpr of HIV-1 (Fontes *et al.*, 2000; Pumroy and Cingolani, 2015). In the same way, importin  $\alpha 3$  is capable

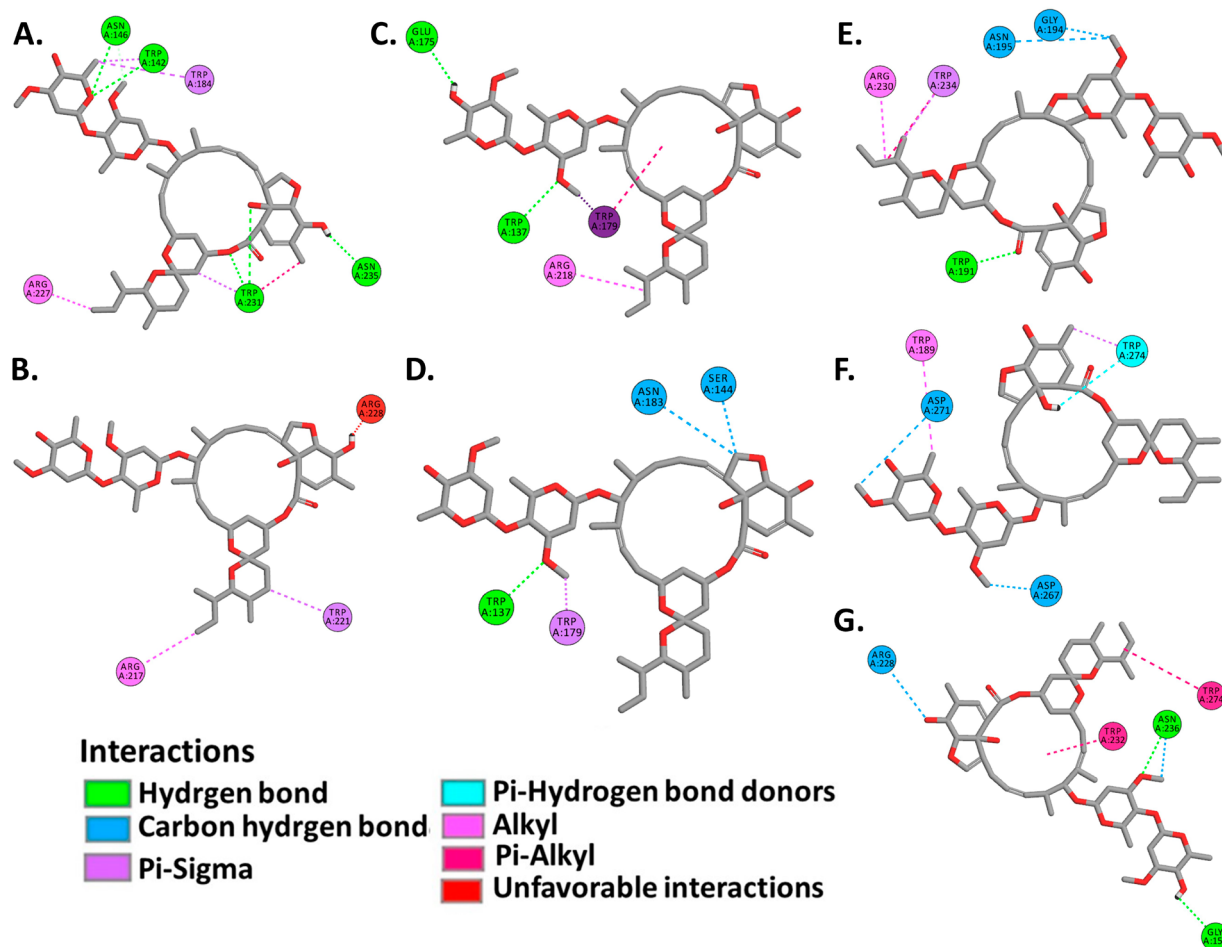


**Figure 7.** Complexes of ivermectin and importin  $\alpha$  isoforms. **A.** Importin  $\alpha 1$ . **B.** Importin  $\alpha 8$ . **C.** Importin  $\alpha 3$ . **D.** Importin  $\alpha 4$ . **E.** Importin  $\alpha 5$ . **F.** Importin  $\alpha 6$ . **G.** Importin  $\alpha 7$ .

**Figura 7.** Complejos de ivermectina y las isoformas de importina  $\alpha$ . **A.** Importina  $\alpha 1$ . **B.** Importina  $\alpha 8$ . **C.** Importina  $\alpha 3$ . **D.** Importina  $\alpha 4$ . **E.** Importina  $\alpha 5$ . **F.** Importina  $\alpha 6$ . **G.** Importina  $\alpha 7$ .

to interact with viral proteins such as PB2 polymerase of influenza A virus, capsid proteins of Chikungunya virus, E1 and E2 proteins of HPV virus (Bian and Wilson, 2010; Pumroy and Cingolani, 2015; Pumroy *et al.*, 2015).

Other isoforms such as importin  $\alpha 5$  and importin  $\alpha 7$  form complexes with influenza A protein PB2; recently it was described that importin  $\alpha 6$  and importin  $\alpha 7$  interact with VP24 protein of Ebola virus (Tarendeau *et al.*, 2007; Xu *et al.*, 2014). On the other hand,  $\alpha 3$  subfamily isoforms play an important role in STAT1/STAT2 heterodimers transport during the antiviral host response (Fagerlund *et al.*, 2002; Sekimoto *et al.*, 1997).

In the last decades it was reported that ivermectin is able to block nucleoplasm-cytoplasm traffic of viral proteins of DENaV, HIV-1, WNV, Hepatitis E Virus (HEV), Bovine Herpesvirus I (BoHV-1) and ZIKV avoiding their replicative cycle (Crump, 2017; Mastrangelo *et al.*, 2012; Ōmura and Crump, 2014; Wagstaff *et al.*, 2012; Yang *et al.*, 2020). King *et al.* (2020) reported that ivermectin is also able to disrupt the interaction of human adenovirus viral E1A protein with importin  $\alpha$  without disturbing importin  $\alpha/\beta 1$  interactions.

An *in vitro* study performed by Caly *et al.* (2020), has evidenced that after 48-72 hours of treatment, ivermectin reduced about 5000 fold the presence of replicated SARS-CoV-2 genome in infected Vero/hSLAM cells, finding  $IC_{50}$  values between 2.2-2.8  $\mu M$ , indicating a high antiviral activity.

Researchers suggest that this decrease could be occurring due to an inhibition of importin  $\alpha/\beta 1$  complex activity, and was also hypothesized that ivermectin reacts between each other creating compound complexes that may interfere with viral processes (Caly *et al.*, 2020; Rizzo, 2020).

Active residues identified in ivermectin-importin  $\alpha$  complexes were also described in complexes mentioned above, so they could probably be sharing the same binding site (major binding site) in the evaluated isoforms (Chook and Blobel, 2001) (Figure 3, Figure 4, Figure 7, Supplementary Table S1, Supplementary Table S2). These observations are in agreement with Yang *et al.* (2020), who demonstrated *in vitro* that ivermectin has the ability to interact with ARM domains of importins  $\alpha$  of *Mus musculus*, and may even cause instability of importin  $\alpha/\beta 1$  complexes.

Although interactions between ivermectin and importin  $\alpha$  are widely accepted, several computational studies have shown that this molecule could have other SARS-CoV-2 proteins as target. A recent *in silico* study performed by Azam *et al.* (2020), described that ivermectin demonstrated binding affinities to SARS-CoV-2 Nsp9 protein and to importin  $\alpha$ , evidencing favorable interaction energies, however, importin  $\alpha$  protein model used belongs to *M. musculus*.

In another study of biophysical and computational approach, was were reported binding affinities and interaction stability of ivermectin (avermectin B1a, avermectin B1b) with targets such as Importin  $\alpha 1$  and Importin  $\beta 1$ , as well as viral proteins such as helicase and protease  $M^{PRO}$ , among which according to kinetic parameters evaluated show greater affinities to viral proteins (González-Paz *et al.*, 2021).

Another computational research revealed that ivermectin exhibit higher binding affinities with the complex formed by RNA polymerase (RdRp) and SARS-CoV-2 RNA molecules, establishing ternary complex (Sen Gupta *et al.*, 2022).

Another *in silico* study performed by Bello (2022), revealed that ivermectin could show as possible interaction target SARS-CoV-2 protease 3CLpro and Nsp9 protein. This was also registered by Choudhury *et al.* (2021), who reported favorable binding to SARS-CoV-2 protease, SARS-CoV-2 replicase and host cell TMPRSS2 (Transmembrane Serine Protease 2) protein. In agreement to this, another computational study performed by Saha and Raihan (2021) revealed that ivermectin may also be a suitable inhibitor of interactions between SARS-CoV-2 spike protein and human ACE2 (Angiotensin-Converting Enzyme 2) protein.

The findings presented in this study add to the current knowledge about the possible mechanisms of action of ivermectin against SARS-CoV-2 infection, which may result in the competition for the major binding site (ARM2-ARM4 domain) of the importin  $\alpha$  isoforms by the viral proteins (N and ORF6) and the ivermectin molecules, allowing the decrease of viral replication success and the reduction of the inhibition of the antiviral response of host cells.

## CONCLUSIONS

This research reports for the first time the identification of binding sites (ARM2-ARM4 domains) in human importin  $\alpha$  isoforms shared by the N and ORF6 proteins of SARS-CoV-2 and ivermectin, suggesting it as one of the possible mechanisms of action of ivermectin against SARS-CoV-2 infection. This study leads to new fields of research focused on the exploration of new compounds with antiviral actions against COVID-19, that targets to this classical nucleocytoplasmic transport pathway involved in viral protein traffic and inhibition of antiviral response in infected cells.

## ACKNOWLEDGMENTS

We would like to thank to the Sistema Nacional de Investigadores (SISNI) of the Consejo Nacional de Ciencia y Tecnología (CONACYT), to the Facultad de Ciencias Exactas y Naturales (FACEN) of the Universidad Nacional de Asunción (UNA), and to the Grupo de Investigación en Biología Computacional y Bioinformática Estructural (GIBCBE) from Paraguay.

## CONFLICTS OF INTEREST

Authors declare that they have no conflict of interest.

## REFERENCES

- Addetia, A., Lieberman, N.A.P., Phung, Q., Hsiang, T.-Y., Xie, H., Roychoudhury, P., Shrestha, L., Loprieno, M.A., Huang, M.-L., Gale, M., Jerome, K.R. and Greninger, A.L. 2021. SARS-CoV-2 ORF6 disrupts bidirectional nucleocytoplasmic transport through interactions with Rae1 and Nup98. *mBio* 12: e00065-21. <https://doi.org/10.1128/mBio.00065-21>
- Andersen, K.G., Rambaut, A., Lipkin, W.I., Holmes, E.C. and Garry, R.F. 2020. The proximal origin of SARS-CoV-2. *Nature*

- Medicine 26: 450–452. <https://doi.org/10.1038/s41591-020-0820-9>
- Azam, F., Taban, I.M., Eid, E.E.M., Iqbal, M., Alam, O., Khan, S., Mahmood, D., Anwar, M.J., Khalilullah, H. and Khan, M.U. 2020. An in-silico analysis of ivermectin interaction with potential SARS-CoV-2 targets and host nuclear importin  $\alpha$ . *Journal of Biomolecular Structure and Dynamics*. 40(6): 2851-2864. <https://doi.org/10.1080/07391102.2020.1841028>
- Baumhardt, J. and Chook, Y.M. 2018. Structures of Importins and Exportins, in: Yang, W. (Ed.), *Nuclear-Cytoplasmic Transport, Nucleic Acids and Molecular Biology*. Springer International Publishing, Cham, pp. 113-149. [https://doi.org/10.1007/978-3-319-77309-4\\_6](https://doi.org/10.1007/978-3-319-77309-4_6)
- Bello, M. 2022. Elucidation of the inhibitory activity of ivermectin with host nuclear importin  $\alpha$  and several SARS-CoV-2 targets. *Journal of Biomolecular Structure and Dynamics*. 40: 8375-8383. <https://doi.org/10.1080/07391102.2021.1911857>
- Berman, H.M., Westbrook, J., Feng, Z., Gilliland, G., Bhat, T.N., Weissig, H., Shindyalov, I.N. and Bourne, P.E. 2000. The protein data bank. *Nucleic Acids Res*. 28: 235-242. <https://doi.org/10.1093/nar/28.1.235>
- Bian, X.-L. and Wilson, V.G. 2010. Common importin alpha specificity for papillomavirus E2 proteins. *Virus Research*. 150: 135-137. <https://doi.org/10.1016/j.virusres.2010.02.011>
- Caly, L., Druce, J.D., Catton, M.G., Jans, D.A. and Wagstaff, K.M. 2020. The FDA-approved drug ivermectin inhibits the replication of SARS-CoV-2 in vitro. *Antiviral Research*. 178: 104787. <https://doi.org/10.1016/j.antiviral.2020.104787>
- Ceraolo, C. and Giorgi, F.M. 2020. Genomic variance of the 2019-nCoV coronavirus. *Journal of Medical Virology*. 92: 522-528. <https://doi.org/10.1002/jmv.25700>
- Chang, C., Hou, M.-H., Chang, C.-F., Hsiao, C.-D. and Huang, T. 2014. The SARS coronavirus nucleocapsid protein – Forms and functions. *Antiviral Research*. 103: 39-50. <https://doi.org/10.1016/j.antiviral.2013.12.009>
- Chelliah, V., Blundell, T.L. and Fernández-Recio, J. 2006. Efficient restraints for protein–protein docking by comparison of observed amino acid substitution patterns with those predicted from local Environment. *Journal of Molecular Biology*. 357: 1669-1682. <https://doi.org/10.1016/j.jmb.2006.01.001>
- Chen, Z., Boon, S.S., Wang, M.H., Chan, R.W.Y. and Chan, P.K.S. 2021. Genomic and evolutionary comparison between SARS-CoV-2 and other human coronaviruses. *Journal of Virological Methods*. 289: 114032. <https://doi.org/10.1016/j.jviromet.2020.114032>
- Cheng, T.M.-K., Blundell, T.L. and Fernandez-Recio, J. 2007. pyDock: Electrostatics and desolvation for effective scoring of rigid-body protein–protein docking. *Proteins: Structure, Function, and Bioinformatics*. 68: 503-515. <https://doi.org/10.1002/prot.21419>
- Chook, Y. and Blobel, G. 2001. Karyopherins and nuclear import. *Current Opinion in Structural Biology*. 11: 703-715. [https://doi.org/10.1016/S0959-440X\(01\)00264-0](https://doi.org/10.1016/S0959-440X(01)00264-0)
- Choudhury, A., Das, N.C., Patra, R., Bhattacharya, M., Ghosh, P., Patra, B.C. and Mukherjee, S. 2021. Exploring the binding efficacy of ivermectin against the key proteins of SARS-CoV-2 pathogenesis: an in silico approach. *Future Virology*. 16: 277-291. <https://doi.org/10.2217/fvl-2020-0342>
- Crump, A. 2017. Ivermectin: enigmatic multifaceted 'wonder' drug continues to surprise and exceed expectations. *The Journal of Antibiotics*. 70: 495-505. <https://doi.org/10.1038/ja.2017.11>
- Dallakyan, S. and Olson, A.J. 2015. Small-molecule library screening by docking with PyRx, in: Hempel, J.E., Williams, C.H., Hong, C.C. (Eds.), *Chemical Biology: Methods and Protocols, Methods in Molecular Biology*. Springer, New York, NY, pp. 243-50. [https://doi.org/10.1007/978-1-4939-2269-7\\_19](https://doi.org/10.1007/978-1-4939-2269-7_19)
- David, A., Islam, S., Tankhilevich, E. and Sternberg, M.J.E. 2022. The AlphaFold database of protein structures: A Biologist's Guide. *Journal of Molecular Biology*. 434: 167336. <https://doi.org/10.1016/j.jmb.2021.167336>
- Fagerlund, R., Melén, K., Kinnunen, L. and Julkunen, I. 2002. Arginine/lysine-rich nuclear localization signals mediate interactions between dimeric STATs and Importin  $\alpha$ 5. *Journal of Biological Chemistry*. 277: 30072-30078. <https://doi.org/10.1074/jbc.M202943200>
- Fang, Y., Jang, H.S., Watson, G.W., Wellappili, D.P. and Tyler, B.M. 2017. Distinctive nuclear localization signals in the oomycete *Phytophthora sojae*. *Front. Microbiol*. 8. <https://doi.org/10.3389/fmicb.2017.00010>
- Fontes, M.R.M., Teh, T. and Kobe, B. 2000. Structural basis of recognition of monopartite and bipartite nuclear localization sequences by mammalian importin- $\alpha$ 1. *Journal of Molecular Biology*. 297: 1183-1194. <https://doi.org/10.1006/jmbi.2000.3642>
- Frieman, M., Yount, B., Heise, M., Kopecky-Bromberg, S.A., Palese, P. and Baric, R.S. 2007. Severe acute respiratory syndrome coronavirus ORF6 antagonizes STAT1 function by sequestering nuclear import factors on the rough endoplasmic reticulum/Golgi membrane. *Journal of Virology*. 81: 9812-9824. <https://doi.org/10.1128/JVI.01012-07>
- Fry, M.Y., Saladi, S.M., Cunha, A. and Clemons Jr, W.M. 2021. Sequence-based features that are determinant for tail-anchored membrane protein sorting in eukaryotes. *Traffic*. 22: 306-318. <https://doi.org/10.1111/tra.12809>
- Gabb, H.A., Jackson, R.M. and Sternberg, M.J.E. 1997. Modelling protein docking using shape complementarity, electrostatics and biochemical information. Edited by J. Thornton. *Journal of Molecular Biology*. 272: 106-120. <https://doi.org/10.1006/jmbi.1997.1203>
- Gao, T., Gao, Y., Liu, X., Nie, Z., Sun, H., Lin, K., Peng, H. and Wang, S. 2021. Identification and functional analysis of the SARS-CoV-2 nucleocapsid protein. *BMC Microbiology*. 21: 58. <https://doi.org/10.1186/s12866-021-02107-3>
- Gayozo, E. and Rojas, L. 2021. Interacción in silico de las moléculas Agathisflavona, Amentoflavona y Punicalina con la Importina  $\alpha$ 1 humana. *Revista Colombiana de Biotecnología*. 23: 15-24. <https://doi.org/10.15446/rev.colomb.biote.v23n2.94466>
- González-Paz, L., Hurtado-León, M.L., Lossada, C., Fernández-Materán, F.V., Vera-Villalobos, J., Loroño, M., Paz, J.L., Jeffreys, L. and Alvarado, Y.J. 2021. Comparative study of the interaction of ivermectin with proteins of interest associated with SARS-CoV-2: A computational and biophysical approach. *Biophysical Chemistry*. 278: 106677. <https://doi.org/10.1016/j.bpc.2021.106677>
- Gordon, D.E., Jang, G.M., Bouhaddou, M., Xu, J., Obernier, K., White, K.M., O'Meara, M.J., Rezelj, V.V., Guo, J.Z., Swaney, D.L., Tummino, T.A., Hüttenhain, R., Kaake, R.M., Richards,

- A.L., Tutuncuoglu, B., Foussard, H., Batra, J., Haas, K., Modak, M., Kim, M., Haas, P., Polacco, B.J., Braberg, H., Fabius, J.M., Eckhardt, M., Soucheray, M., Bennett, M.J., Cakir, M., McGregor, M.J., Li, Q., Meyer, B., Roesch, F., Vallet, T., Mac Kain, A., Miorin, L., Moreno, E., Naing, Z.Z.C., Zhou, Y., Peng, S., Shi, Y., Zhang, Z., Shen, W., Kirby, I.T., Melnyk, J.E., Chorba, J.S., Lou, K., Dai, S.A., Barrio-Hernandez, I., Memon, D., Hernandez-Armenta, C., Lyu, J., Mathy, C.J.P., Perica, T., Pilla, K.B., Ganesan, S.J., Saltzberg, D.J., Rakesh, R., Liu, X., Rosenthal, S.B., Calviello, L., Venkataramanan, S., Liboy-Lugo, J., Lin, Y., Huang, X.-P., Liu, Y., Wankowicz, S.A., Bohn, M., Safari, M., Ugur, F.S., Koh, C., Savar, N.S., Tran, Q.D., Shengjuler, D., Fletcher, S.J., O'Neal, M.C., Cai, Y., Chang, J.C.J., Broadhurst, D.J., Klippsten, S., Sharp, P.P., Wenzell, N.A., Kuzuoglu-Ozturk, D., Wang, H.-Y., Trenker, R., Young, J.M., Cavero, D.A., Hiatt, J., Roth, T.L., Rathore, U., Subramanian, A., Noack, J., Hubert, M., Stroud, R.M., Frankel, A.D., Rosenberg, O.S., Verba, K.A., Agard, D.A., Ott, M., Emerman, M., Jura, N., von Zastrow, M., Verdin, E., Ashworth, A., Schwartz, O., d'Enfert, C., Mukherjee, S., Jacobson, M., Malik, H.S., Fujimori, D.G., Ideker, T., Craik, C.S., Floor, S.N., Fraser, J.S., Gross, J.D., Sali, A., Roth, B.L., Ruggero, D., Taunton, J., Kortemme, T., Beltrao, P., Vignuzzi, M., García-Sastre, A., Shokat, K.M., Shoichet, B.K. and Krogan, N.J. 2020. A SARS-CoV-2 protein interaction map reveals targets for drug repurposing. *Nature*. 583: 459-468. <https://doi.org/10.1038/s41586-020-2286-9>
- Grosdidier, S., Pons, C., Solernou, A. and Fernández-Recio, J. 2007. Prediction and scoring of docking poses with pyDock. *Proteins: Structure, Function, and Bioinformatics*. 69: 852-858. <https://doi.org/10.1002/prot.21796>
- Hanwell, M.D., Curtis, D.E., Lonie, D.C., Vandermeersch, T., Zurek, E. and Hutchison, G.R. 2012. Avogadro: an advanced semantic chemical editor, visualization, and analysis platform. *J. Cheminform.* 4: 17. <https://doi.org/10.1186/1758-2946-4-17>
- He, R., Dobie, F., Ballantine, M., Leeson, A., Li, Y., Bastien, N., Cutts, T., Andonov, A., Cao, J., Booth, T.F., Plummer, F.A., Tyler, S., Baker, L. and Li, X. 2004. Analysis of multimerization of the SARS coronavirus nucleocapsid protein. *Biochemical and Biophysical Research Communications*. 316: 476-483. <https://doi.org/10.1016/j.bbrc.2004.02.074>
- Heo, L., Lee, H. and Seok, C. 2016. GalaxyRefineComplex: Refinement of protein-protein complex model structures driven by interface repacking. *Sci Rep*. 6: 32153. <https://doi.org/10.1038/srep32153>
- Horton, P., Park, K.-J., Obayashi, T., Fujita, N., Harada, H., Adams-Collier, C.J. and Nakai, K. 2007. WoLF PSORT: protein localization predictor. *Nucleic Acids Res.* 35: W585-W587. <https://doi.org/10.1093/nar/gkm259>
- Hussain, S. and Gallagher, T. 2010. SARS-coronavirus protein 6 conformations required to impede protein import into the nucleus. *Virus Research*. 153: 299-304. <https://doi.org/10.1016/j.virusres.2010.08.017>
- Ibrahim, I.M., Abdelmalek, D.H., Elshahat, M.E. and Elfiky, A.A. 2020. COVID-19 spike-host cell receptor GRP78 binding site prediction. *Journal of Infection* 80: 554-562. <https://doi.org/10.1016/j.jinf.2020.02.026>
- Iqbal, H.M.N., Romero-Castillo, K.D., Bilal, M. and Parra-Saldivar, R. 2020. The emergence of novel-coronavirus and its replication cycle - An overview. *Journal of Pure and Applied Microbiology*. 14(1): 13-16. <https://doi.org/10.22207/JPAM.14.1.03>
- Jiménez-García, B., Pons, C. and Fernández-Recio, J. 2013. pyDockWEB: a web server for rigid-body protein-protein docking using electrostatics and desolvation scoring. *Bioinformatics*. 29: 1698-1699. <https://doi.org/10.1093/bioinformatics/btt262>
- Jumper, J., Evans, R., Pritzel, A., Green, T., Figurnov, M., Ronneberger, O., Tunyasuvunakool, K., Bates, R., Židek, A., Potapenko, A., Bridgland, A., Meyer, C., Kohl, S.A.A., Ballard, A.J., Cowie, A., Romera-Paredes, B., Nikolov, S., Jain, R., Adler, J., Back, T., Petersen, S., Reiman, D., Clancy, E., Zielinski, M., Steinegger, M., Pacholska, M., Berghammer, T., Bodenstein, S., Silver, D., Vinyals, O., Senior, A.W., Kavukcuoglu, K., Kohli, P. and Hassabis, D. 2021. Highly accurate protein structure prediction with AlphaFold. *Nature*. 596: 583-589. <https://doi.org/10.1038/s41586-021-03819-2>
- Kannan, S., Shaik Syed Ali, P., Sheeza, A. and Hemalatha, K. 2020. COVID-19 (Novel Coronavirus 2019) - recent trends. *Eur Rev Med Pharmacol Sci*. 24: 2006-2011. [https://doi.org/10.26355/eurrev\\_202002\\_20378](https://doi.org/10.26355/eurrev_202002_20378)
- Kato, K., Ikliptikawati, D.K., Kobayashi, A., Kondo, H., Lim, K., Hazawa, M. and Wong, R.W. 2021. Overexpression of SARS-CoV-2 protein ORF6 dislocates RAE1 and NUP98 from the nuclear pore complex. *Biochemical and Biophysical Research Communications*. 536: 59-66. <https://doi.org/10.1016/j.bbrc.2020.11.115>
- Kim, S., Thiessen, P.A., Bolton, E.E., Chen, J., Fu, G., Gindulyte, A., Han, L., He, J., He, S., Shoemaker, B.A., Wang, J., Yu, B., Zhang, J. and Bryant, S.H. 2016. PubChem substance and compound databases. *Nucleic Acids Res.* 44: D1202-D1213. <https://doi.org/10.1093/nar/gkv951>
- King, C.R., Tessier, T.M., Dodge, M.J., Weinberg, J.B. and Mymryk, J.S. 2020. Inhibition of human adenovirus replication by the importin  $\alpha/\beta 1$  nuclear import inhibitor ivermectin. *Journal of Virology*. 94: e00710-e00720. <https://doi.org/10.1128/JVI.00710-20>
- Kopecky-Bromberg, S.A., Martínez-Sobrido, L., Frieman, M., Baric, R.A. and Palese, P. 2007. Severe acute respiratory syndrome coronavirus open reading frame (ORF) 6, and nucleocapsid proteins function as interferon antagonists. *Journal of Virology*. 81: 548-557. <https://doi.org/10.1128/JVI.01782-06>
- Kumar, S., Stecher, G., Li, M., Knyaz, C. and Tamura, K. 2018. MEGA X: Molecular evolutionary genetics analysis across computing platforms. *Mol Biol Evol*. 35: 1547-1549. <https://doi.org/10.1093/molbev/msy096>
- Kyte, J. and Doolittle, R.F. 1982. A simple method for displaying the hydropathic character of a protein. *Journal of Molecular Biology*. 157: 105-132. [https://doi.org/10.1016/0022-2836\(82\)90515-0](https://doi.org/10.1016/0022-2836(82)90515-0)
- Laskowski, R.A., MacArthur, M.W., Moss, D.S. and Thornton, J.M. 1993. PROCHECK: a program to check the stereochemical quality of protein structures. *J. Appl. Cryst.* 26: 283-291. <https://doi.org/10.1107/S0021889892009944>
- Li, J.-Y., Liao, C.-H., Wang, Q., Tan, Y.-J., Luo, R., Qiu, Y. and Ge, X.-Y. 2020. The ORF6, ORF8 and nucleocapsid proteins of SARS-CoV-2 inhibit type I interferon signaling pathway. *Virus Research*. 286: 198074. <https://doi.org/10.1016/j.virusres.2020.198074>
- Li, W., Cowley, A., Uludag, M., Gur, T., McWilliam, H., Squizzato, S., Park, Y.M., Buso, N. and Lopez, R. 2015. The EMBL-EBI bioinformatics web and programmatic tools framework.

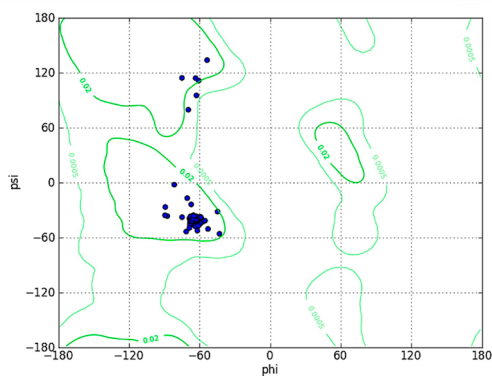
- Nucleic Acids Res. 43: W580-W584. <https://doi.org/10.1093/nar/gkv279>
- Liu, D.X., Fung, T.S., Chong, K.K.-L., Shukla, A. and Hilgenfeld, R. 2014. Accessory proteins of SARS-CoV and other coronaviruses. *Antiviral Research*. 109: 97-109. <https://doi.org/10.1016/j.antiviral.2014.06.013>
- Lu, R., Zhao, X., Li, J., Niu, P., Yang, B., Wu, H., Wang, W., Song, H., Huang, B., Zhu, N., Bi, Y., Ma, X., Zhan, F., Wang, L., Hu, T., Zhou, H., Hu, Z., Zhou, W., Zhao, L., Chen, J., Meng, Y., Wang, J., Lin, Y., Yuan, J., Xie, Z., Ma, J., Liu, W.J., Wang, D., Xu, W., Holmes, E.C., Gao, G.F., Wu, G., Chen, W., Shi, W. and Tan, W. 2020. Genomic characterisation and epidemiology of 2019 novel coronavirus: implications for virus origins and receptor binding. *The Lancet*. 395: 565-574. [https://doi.org/10.1016/S0140-6736\(20\)30251-8](https://doi.org/10.1016/S0140-6736(20)30251-8)
- Mastrangelo, E., Pezzullo, M., De Burghgraeve, T., Kaptein, S., Pastorino, B., Dallmeier, K., de Lamballerie, X., Neyts, J., Hanson, A.M., Frick, D.N., Bolognesi, M. and Milani, M. 2012. Ivermectin is a potent inhibitor of flavivirus replication specifically targeting NS3 helicase activity: new prospects for an old drug. *J. Antimicrob Chemother*. 67: 1884-1894. <https://doi.org/10.1093/jac/dks147>
- Mirdita, M., Schütze, K., Moriwaki, Y., Heo, L., Ovchinnikov, S. and Steinegger, M. 2022. ColabFold: making protein folding accessible to all. *Nat Methods*. 19: 679-682. <https://doi.org/10.1038/s41592-022-01488-1>
- Miyamoto, Y., Itoh, Y., Suzuki, T., Tanaka, T., Sakai, Y., Koido, M., Hata, C., Wang, C.-X., Otani, M., Moriishi, K., Tachibana, T., Kamatani, Y., Yoneda, Y., Okamoto, T. and Oka, M. 2022. SARS-CoV-2 ORF6 disrupts nucleocytoplasmic trafficking to advance viral replication. *Commun Biol*. 5: 1-15. <https://doi.org/10.1038/s42003-022-03427-4>
- Narayanan, K., Huang, C. and Makino, S. 2008. SARS coronavirus accessory proteins. *Virus Research, SARS-CoV Pathogenesis and Replication*. 133: 113-121. <https://doi.org/10.1016/j.virusres.2007.10.009>
- Ōmura, S. and Crump, A. 2014. Ivermectin: panacea for resource-poor communities? *Trends in Parasitology*. 30: 445-455. <https://doi.org/10.1016/j.pt.2014.07.005>
- Pallara, C., Jiménez-García, B., Romero, M., Moal, I.H. and Fernández-Recio, J. 2017. pyDock scoring for the new modeling challenges in docking: Protein-peptide, homo-multimers, and domain-domain interactions. *Proteins: Structure, Function, and Bioinformatics*. 85: 487-496. <https://doi.org/10.1002/prot.25184>
- Pettersen, E.F., Goddard, T.D., Huang, C.C., Couch, G.S., Greenblatt, D.M., Meng, E.C. and Ferrin, T.E. 2004. UCSF Chimera—A visualization system for exploratory research and analysis. *Journal of Computational Chemistry*. 25: 1605-1612. <https://doi.org/10.1002/jcc.20084>
- Pumroy, R. and Cingolani, G. 2015. Diversification of importin- $\alpha$  isoforms in cellular trafficking and disease states. *Biochemical Journal*. 466 (1): 13-28. <https://doi.org/10.1042/BJ20141186>
- Pumroy, R.A., Ke, S., Hart, D.J., Zachariae, U. and Cingolani, G. 2015. Molecular determinants for nuclear import of influenza A PB2 by importin  $\alpha$  isoforms 3 and 7. *Structure*. 23: 374-384. <https://doi.org/10.1016/j.str.2014.11.015>
- Qin, Z., Jinming, C., Xiaojun, H., Huanying, Z., Jicheng, H., Ling, F., Kunpeng, L. and Jingqiang, Z. 2004. The life cycle of SARS coronavirus in Vero E6 cells. *Journal of Medical Virology*. 73: 332-337. <https://doi.org/10.1002/jmv.20095>
- Rizzo, E. 2020. Ivermectin, antiviral properties and COVID-19: a possible new mechanism of action. *Naunyn-Schmiedeberg's Arch Pharmacol*. 393: 1153-1156. <https://doi.org/10.1007/s00210-020-01902-5>
- Robert, X. and Gouet, P. 2014. Deciphering key features in protein structures with the new ENDscript server. *Nucleic Acids Res*. 42: W320-W324. <https://doi.org/10.1093/nar/gku316>
- Rowland, R.R.R., Chauhan, V., Fang, Y., Pekosz, A., Kerrigan, M. and Burton, M.D. 2005. Intracellular localization of the severe acute respiratory syndrome Ccoronavirus nucleocapsid protein: Absence of nucleolar accumulation during infection and after expression as a recombinant protein in Vero cells. *Journal of Virology*. 79: 11507-11512. <https://doi.org/10.1128/JVI.79.17.11507-11512.2005>
- Saha, J.K. and Raihan, Md.J. 2021. The binding mechanism of ivermectin and levosalbutamol with spike protein of SARS-CoV-2. *Struct Chem*. 32: 1985-1992. <https://doi.org/10.1007/s11224-021-01776-0>
- Sekimoto, T., Imamoto, N., Nakajima, K., Hirano, T. and Yoneda, Y. 1997. Extracellular signal-dependent nuclear import of Stat1 is mediated by nuclear pore-targeting complex formation with NPI-1, but not Rch1. *The EMBO Journal*. 16: 7067-7077. <https://doi.org/10.1093/emboj/16.23.7067>
- Sen Gupta, P.S., Biswal, S., Panda, S.K., Ray, A.K. and Rana, M.K. 2022. Binding mechanism and structural insights into the identified protein target of COVID-19 and importin- $\alpha$  with in-vitro effective drug ivermectin. *Journal of Biomolecular Structure and Dynamics*. 40: 2217-2226. <https://doi.org/10.1080/07391102.2020.1839564>
- Shereen, M.A., Khan, S., Kazmi, A., Bashir, N. and Siddique, R. 2020. COVID-19 infection: Origin, transmission, and characteristics of human coronaviruses. *Journal of Advanced Research*. 24: 91-98. <https://doi.org/10.1016/j.jare.2020.03.005>
- Sievers, F. and Higgins, D.G. 2014. Clustal omega, accurate alignment of very large numbers of sequences, in: Russell, D.J. (Ed.), *Multiple Sequence Alignment Methods, Methods in Molecular Biology*. Humana Press, Totowa, NJ, pp. 105-116. [https://doi.org/10.1007/978-1-62703-646-7\\_6](https://doi.org/10.1007/978-1-62703-646-7_6)
- Surjit, M., Liu, B., Jameel, S., Chow, V.T.K. and Lal, S.K. 2004. The SARS coronavirus nucleocapsid protein induces actin reorganization and apoptosis in COS-1 cells in the absence of growth factors. *Biochem J*. 383: 13-18. <https://doi.org/10.1042/BJ20040984>
- Tarendeau, F., Boudet, J., Guilligay, D., Mas, P.J., Bougault, C.M., Boulo, S., Baudin, F., Ruigrok, R.W.H., Daigle, N., Ellenberg, J., Cusack, S., Simorre, J.-P. and Hart, D.J. 2007. Structure and nuclear import function of the C-terminal domain of influenza virus polymerase PB2 subunit. *Nat Struct Mol Biol*. 14: 229-233. <https://doi.org/10.1038/nsmb1212>
- Timani, K.A., Liao, Q., Ye, Linbai, Zeng, Y., Liu, J., Zheng, Y., Ye, Li, Yang, X., Lingbao, K., Gao, J. and Zhu, Y. 2005. Nuclear/nucleolar localization properties of C-terminal nucleocapsid protein of SARS coronavirus. *Virus Research*. 114: 23-34. <https://doi.org/10.1016/j.virusres.2005.05.007>
- Trott, O. and Olson, A.J. 2010. AutoDock Vina: Improving the speed and accuracy of docking with a new scoring function, efficient optimization, and multithreading. *Journal of Computational Chemistry*. 31: 455-461. <https://doi.org/10.1002/jcc.21334>
- Vangone, A., Schaarschmidt, J., Koukos, P., Geng, C., Citro, N., Trellet, M.E., Xue, L.C. and Bonvin, A.M.J.J. 2019. Large-

- scale prediction of binding affinity in protein–small ligand complexes: the PRODIGY-LIG web server. *Bioinformatics*. 35: 1585-1587. <https://doi.org/10.1093/bioinformatics/bty816>
- Varadi, M., Anyango, S., Deshpande, M., Nair, S., Natassia, C., Yordanova, G., Yuan, D., Stroe, O., Wood, G., Laydon, A., Židek, A., Green, T., Tunyasuvunakool, K., Petersen, S., Jumper, J., Clancy, E., Green, R., Vora, A., Lutfi, M., Figurnov, M., Cowie, A., Hobbs, N., Kohli, P., Kleywegt, G., Birney, E., Hassabis, D. and Velankar, S. 2022. AlphaFold Protein Structure Database: massively expanding the structural coverage of protein-sequence space with high-accuracy models. *Nucleic Acids Research*. 50: D439-D444. <https://doi.org/10.1093/nar/gkab1061>
- Wagstaff, K.M., Sivakumaran, H., Heaton, S.M., Harrich, D. and Jans, D.A. 2012. Ivermectin is a specific inhibitor of importin  $\alpha/\beta$ -mediated nuclear import able to inhibit replication of HIV-1 and dengue virus. *Biochemical Journal*. 443: 851-856. <https://doi.org/10.1042/BJ20120150>
- Williams, C.J., Headd, J.J., Moriarty, N.W., Prisant, M.G., Videau, L.L., Deis, L.N., Verma, V., Keedy, D.A., Hintze, B.J., Chen, V.B., Jain, S., Lewis, S.M., Arendall III, W.B., Snoeyink, J., Adams, P.D., Lovell, S.C., Richardson, J.S. and Richardson, D.C. 2018. MolProbity: More and better reference data for improved all-atom structure validation. *Protein Science*. 27: 293-315. <https://doi.org/10.1002/pro.3330>
- Wu, F., Zhao, S., Yu, B., Chen, Y.-M., Wang, W., Song, Z.-G., Hu, Y., Tao, Z.-W., Tian, J.-H., Pei, Y.-Y., Yuan, M.-L., Zhang, Y.-L., Dai, F.-H., Liu, Y., Wang, Q.-M., Zheng, J.-J., Xu, L., Holmes, E.C. and Zhang, Y.-Z. 2020. A new coronavirus associated with human respiratory disease in China. *Nature*. 579: 265-269. <https://doi.org/10.1038/s41586-020-2008-3>
- Wulan, W.N., Heydet, D., Walker, E.J., Gahan, M.E. and Ghildyal, R. 2015. Nucleocytoplasmic transport of nucleocapsid proteins of enveloped RNA viruses. *Front. Microbiol.* 6. <https://doi.org/10.3389/fmicb.2015.00553>
- Wurm, T., Chen, H., Hodgson, T., Britton, P., Brooks, G. and Hiscox, J.A. 2001. Localization to the nucleolus is a common feature of coronavirus nucleoproteins, and the protein may disrupt host cell division. *Journal of Virology*. 75: 9345-9356. <https://doi.org/10.1128/JVI.75.19.9345-9356.2001>
- Xu, W., Edwards, M.R., Borek, D.M., Feagins, A.R., Mittal, A., Alinger, J.B., Berry, K.N., Yen, B., Hamilton, J., Brett, T.J., Pappu, R.V., Leung, D.W., Basler, C.F. and Amarasinghe, G.K. 2014. Ebola virus VP24 targets a unique NLS binding site on karyopherin alpha 5 to selectively compete with nuclear import of phosphorylated STAT1. *Cell Host & Microbe*. 16: 187-200. <https://doi.org/10.1016/j.chom.2014.07.008>
- Yang, S.N.Y., Atkinson, S.C., Wang, C., Lee, A., Bogoyevitch, M.A., Borg, N.A. and Jans, D.A. 2020. The broad spectrum antiviral ivermectin targets the host nuclear transport importin  $\alpha/\beta$  heterodimer. *Antiviral Research*. 177: 104760. <https://doi.org/10.1016/j.antiviral.2020.104760>
- Ye, Z., Wong, C.K., Li, P. and Xie, Y. 2008. A SARS-CoV protein, ORF-6, induces caspase-3 mediated, ER stress and JNK-dependent apoptosis. *Biochimica et Biophysica Acta (BBA) - General Subjects*. 1780: 1383-1387. <https://doi.org/10.1016/j.bbagen.2008.07.009>
- Zaidi, A.K. and Dehgani-Mobaraki, P. 2022. The mechanisms of action of ivermectin against SARS-CoV-2—an extensive review. *J Antibiot.* 75: 60-71. <https://doi.org/10.1038/s41429-021-00491-6>
- Zhao, J., Falcón, A., Zhou, H., Netland, J., Enjuanes, L., Breña, P.P. and Perlman, S. 2009. Severe acute respiratory syndrome coronavirus protein 6 is required for optimal replication. *Journal of Virology*. 83: 2368-2373. <https://doi.org/10.1128/JVI.02371-08>
- Zhou, P., Yang, X.L., Wang, X.G., Hu, B., Zhang, L., Zhang, W., Si, H.R., Zhu, Y., Li, B., Huang, C.L., Chen, H.D., Chen, J., Luo, Y., Guo, H., Jiang, R.D., Liu, M.Q., Chen, Y., Shen, X.R., Wang, X., Zheng, X.S., Zhao, K., Chen, Q.J., Deng, F., Liu, L.L., Yan, B., Zhan, F.X., Wang, Y.Y., Xiao, G.F. and Shi, Z.L. 2020. A pneumonia outbreak associated with a new coronavirus of probable bat origin. *Nature*. 579: 270-273. <https://doi.org/10.1038/s41586-020-2012-7>

S1. Supplementary Figure 1

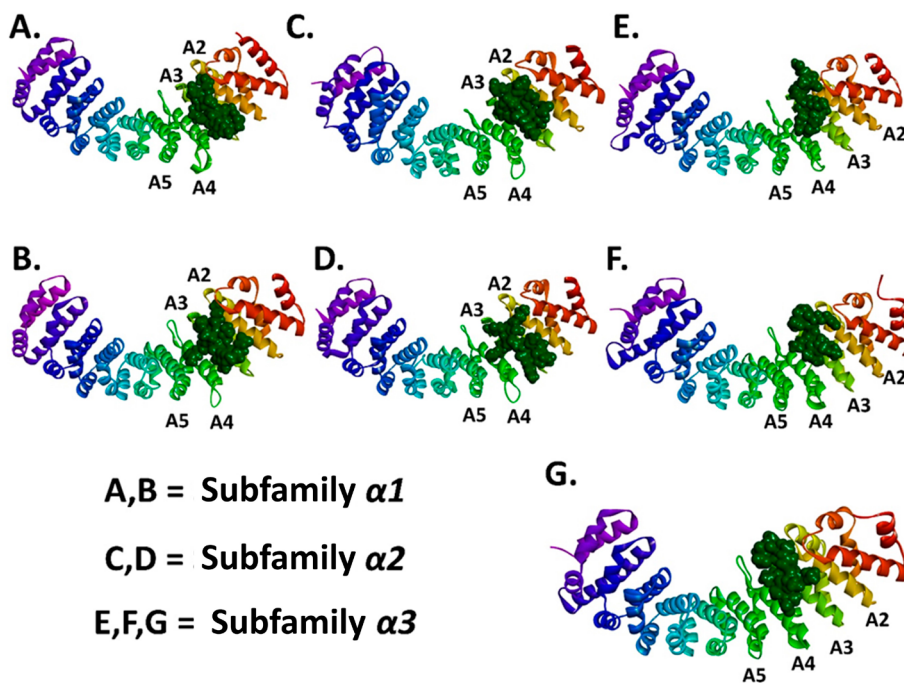
S1. Figura suplementaria 1

<b>Protein Geometry</b>	<b>Poor rotamers</b>	<b>0</b>	<b>0%</b>	<b>Goal: &lt;0.3%</b>
	<b>Favored rotamers</b>	<b>60</b>	<b>100%</b>	<b>Goal: &gt;98%</b>
	<b>Ramachandran outliers</b>	<b>0</b>	<b>0%</b>	<b>Goal: &lt;0.05%</b>
	<b>Ramachandran favored</b>	<b>55</b>	<b>93.22%</b>	<b>Goal: &gt;98%</b>
	<b>Rama distribution Z-score</b>	<b>1.28±0.99</b>		<b>Goal: abs(Z-score)&lt;2</b>
	<b>Cβ deviations &gt;0.25Å</b>	<b>0</b>	<b>0%</b>	<b>Goal: 0</b>
	<b>Bad bonds</b>	<b>0/518</b>	<b>0%</b>	<b>Goal: 0%</b>
<b>Peptide Omegas</b>	<b>Bad angles</b>	<b>5/700</b>	<b>0.71%</b>	<b>Goal: &lt;0.1%</b>
	<b>Cis Prolines</b>	<b>0/1</b>	<b>0%</b>	<b>Expected: ≤1 per chain. or ≤5%</b>
<b>Additional validations</b>	<b>Chiral volume outliers</b>	<b>0/85</b>		
	<b>Waters with clashes</b>	<b>0/0</b>	<b>0%</b>	



S2. Supplementary Figure 2

S2. Figura suplementaria 2



S3. Supplementary Figure 3  
S3. Figura suplementaria 3

